ESTIMATING THE POSITION OF AN IMAGE WITH UNKNOWN INTENSITY SHAPE

Yury E. Korchagin[1], Viacheslav N. Vereshchagin[1], Alexander V. Terekhov[2], Kirill A. Melnikov[2,3,*]

[1]Department of Radio Physics, Voronezh State University, Voronezh, Russia
[2]Department of Electronics and Nanoelectronics, National Research University "Moscow Power Engineering Institute", Moscow, Russia
[3]International Laboratory of Statistics of Stochastic Processes and Quantitative Finance, National Research Tomsk State University, Tomsk, Russia

*E-mail of corresponding author: kirill.a.melnikov@mail.ru

Resume
The problem considered is to estimate the image position of a spatially extended object. It is assumed that the shape of the image intensity is a priori unknown, but it can be predicted with some error. In order to synthesize the estimate of the image position, the quasi-likelihood version of the maximum likelihood method is used. Behavior of the signal function in the neighborhood of the real image position is studied. Characteristics of the resulting estimate, such as bias and dispersion, are found by means of the local Markov approximation method. Influence of non-uniformity of the received image intensity upon the estimate accuracy is demonstrated by an example of receiving the rectangular image with linearly varying intensity.

Article info
Received 19 May 2020
Accepted 12 June 2020
Online 6 November 2020

Keywords:
image processing,
unknown intensity,
estimate of position,
quasi-likelihood approach,
local Markov approximation method,
characteristics of estimate

Available online: https://doi.org/10.26552/com.C.2021.1.C15-C22

ISSN 1335-4205 (print version)
ISSN 2585-7878 (online version)

1 Introduction

Systems for estimating (predicting) the position of a spatially extended object by its own image are widely used for security purposes, traffic monitoring and management, in railway transport and in other sectors [1-4]. However, the information processing algorithms, applied in the specified systems, can often provide the simplest operations only, such as detection of a moving object against a relatively simple background with a subsequent measurement of its speed. Thus, such systems, in fact, are video surveillance systems and not the measuring ones. A more complicated task is when realization of the two-dimensional random field $\xi(x,y)$ is processed, which, in general case, includes the image of an object with unknown coordinates to be measured, the background and the spatial noise [2-5]. The useful image is often described by a quasi-deterministic function $s(x,y)$ of the two variables determining the dependence of the image intensity upon the coordinates (x,y). One can call $s(x,y)$ the intensity distribution or the intensity profile of the image.

Depending on both the nature of the image and the resolution of the receiving system, the function $s(x,y)$ may be a regular or discontinuous one [5]. Discontinuous functions describe objects with well-defined boundaries.

Some tasks of optimal and suboptimal image processing of the spatially extended objects, with the statistical nature of the observed field $\xi(x,y)$ taken into account, are considered in [2-10]. It is presupposed that the useful image is distorted by both the spatial noise and the additive or applicative background. When using the additive model of interaction between the image and the background, the intensities of the quasi-deterministic image and the background are different from zero within the area occupied by the image. However, in the case of the applicative model use, the image shadows background, i.e. the background intensity is zero within the area occupied by the image. Algorithms for detecting the quasi-deterministic image in the presence of a background are studied in [8], while in [9-10] algorithms for processing the image with unknown position, observed in the presence of the additive Gaussian spatial white noise, are developed. In particular, in [10], efficiency of the non-uniform image position estimate is tested for the case when the image intensity distribution is a priori known. However, in practice, there may be cases where the image intensity distribution is unknown. Thus, it is of interest to consider a more general case including estimating the position of the image with an unknown varying intensity.

In order to estimate the image position, the quasi-likelihood (QL) measurer can be applied that is synthesized for some predicted (presupposed) intensity distribution of the image of the same shape and area. In this paper, both

© 2021 UNIVERSITY OF ZILINA

synthesis and analysis of the QL algorithm for estimating the unknown position of the two-dimensional signal (image) with the unknown intensity distribution are carried out. Influence with a priori ignorance of the image parameters upon the efficiency of the resulting estimate is studied.

2 The problem statement

The image with the unknown intensity and position can be described by the function [5, 7-10]

$$s(x,y,\lambda,\eta) = f(x-\lambda, y-\eta) I(x-\lambda, y-\eta), \tag{1}$$

where $f(x,y)$ is the function differentiable in both arguments that describes the intensity distribution, while λ and η are values characterizing the image position in the plane two-dimensional observation area Ω. Equation (1) occupies the area $\Omega_s(\lambda,\eta) \subset \Omega$ described by the indicator function

$$\begin{aligned} I(x,y) &= \begin{cases} 1, & x,y \in \Omega_s(0,0), \\ 0, & x,y \notin \Omega_s(0,0), \end{cases} \\ I(x-\lambda, y-\eta) &= \begin{cases} 1, & x,y \in \Omega_s(\lambda,\eta), \\ 0, & x,y \notin \Omega_s(\lambda,\eta). \end{cases} \end{aligned} \tag{2}$$

Let the realization of the Gaussian random field

$$\xi(x,y) = s(x,y,\lambda_0,\eta_0) + n(x,y), \quad x,y \in \Omega \tag{3}$$

be observed within the area Ω. Here λ_0 and η_0 are the unknown position parameters and $n(x,y)$ is the spatial Gaussian white noise with zero mathematical expectation and the one-side spectral density N_0.

In the observation area Ω, one chooses the coordinate system so that the equality [9-10]

$$\iint\limits_{\Omega} xI(x,y)dxdy = \iint\limits_{\Omega} yI(x,y)dxdy \tag{4}$$

is satisfied, that is, the origin is located in the centre of the area $\Omega_s(0,0)$ described by the indicator $I(x,y)$. Then λ and η are coordinates of the centre of the area $\Omega_s(\lambda,\eta)$ occupied by the image and described by the indicator function $I(x-\lambda, y-\eta)$, while λ_0 and η_0 are the unknown real coordinates of the centre of the image presented in the observable realization in Equation (3), they determine its position.

Let it be assumed that the parameter η_0 is a priori known. Then, without loss of generality, one can presume that $\eta_0 = 0$ and rewrite expressions (3) and (1) as follows

$$\xi(x,y) = s(x,y,\lambda_0) + n(x,y), \quad x,y \in \Omega, \tag{5}$$

$$s(x,y,\lambda) = f(x-\lambda, y) I(x-\lambda, y). \tag{6}$$

The abscissa λ_0 of the centre of the area $\Omega_s(\lambda_0,0) \equiv \Omega_s(\lambda,y)$, occupied by the image, is a priori unknown. Let it takes values from the interval $[-\lambda_{\max}/2, \lambda_{\max}/2]$. By observations in Equation (5), it is necessary to estimate the unknown position λ_0 of the image $s(x,y,\lambda_0)$ with the unknown intensity distribution $f(x,y)$.

3 The estimation algorithm synthesis

If the distribution intensity $f(x,y)$ of Equation (6) is known, then it is possible to find the logarithm of the functional of the likelihood ratio (FLR) and then develop the maximum likelihood (ML) estimation algorithm. According to the ML method [11-12], in order to obtain an estimate $\hat{\lambda}$ of the position λ_0 of Equation (6), it is necessary to form the component of the FLR logarithm depending on the current value λ of the unknown parameter λ_0 as follows [13-14]

$$\begin{aligned} L_m(\lambda) &= \frac{2}{N_0} \iint\limits_{\Omega} \xi(x,y) s(x,y,\lambda) dxdy, \\ &\lambda \in [-\lambda_{\max}/2, \lambda_{\max}/2]. \end{aligned} \tag{7}$$

The ML estimate λ_m of the image position coincides with the position of the greatest maximum of the decision statistics in Equation (7), that is, $\lambda_m = \arg\sup L_m(\lambda)$.

If the image intensity $f(x,y)$ is a priori unknown, then one can use the estimation algorithm synthesized for some presupposed image intensity distribution $g(x,y) \geq 0$. Then, the output of the receiver produces some function

$$L(\lambda) = \frac{2}{N_0} \iint\limits_{\Omega} \xi(x,y) \tilde{s}(x,y,\lambda) dxdy. \tag{8}$$

Here $\tilde{s}(x,y)$ is the reference image and, in general case, $f(x,y) \neq g(x,y)$. The QL algorithm, for finding the estimate $\hat{\lambda}$ of the position λ_0, includes the search of the position of the greatest maximum of the signal in Equation (8) at the receiver output:

$$\hat{\lambda} = \arg\sup L(\lambda), \quad \lambda \in [-\lambda_{\max}/2, \lambda_{\max}/2]. \tag{9}$$

If the function $f(x,y)$ is a priori known so that

$$f(x,y) = g(x,y), \tag{10}$$

then Equation (8) coincides with the FLR logarithm when implementing the optimal reception in Equation (7) and the QL estimate in Equation (9) coincides with the ML estimate λ_m.

4 The statistical characteristics of the decision statistics

In order to determine the characteristics of the QL estimate in Equation (9), the statistical properties of the decision statistics in Equation (8) are examined. By substituting Equation (3) into Equation (8), the functional in Equation (8) is presented as the sum of signal and noise components [12]:

$$L(\lambda,\lambda_0) = S(\lambda,\lambda_0) + N(\lambda). \tag{11}$$

Here

$$S(\lambda,\lambda_0) = \frac{2}{N_0}\iint\limits_{\Omega} f(x-\lambda_0,y)g(x-\lambda,y)\cdot \\ \cdot I(x-\lambda_0,y)I(x-\lambda,y)dxdy, \tag{12}$$

$$N(\lambda) = \frac{2}{N_0}\iint\limits_{\Omega} n(x,y)g(x-\lambda,y)I(x-\lambda,y)dxdy \tag{13}$$

are the signal and noise components, respectively.

Similarly to [15], let it be supposed that in the neighborhood of the point λ_0 the signal function satisfies the conditions

$$S(\lambda,\lambda_0) > 0,\ dS(\lambda,\lambda_0)/d\lambda|_{\lambda=\lambda_0+0} < 0, \\ d(\lambda,\lambda_0)/d\lambda|_{\lambda=\lambda_0+0} > 0, \tag{14}$$

while the functions $f(x,y)$ and $g(x,y)$ do not vanish at the boundary of the area $\Omega_S(\lambda,\eta)$. Then, position of the maximum of the signal function $S(\lambda,\lambda_0)$ by the variable λ coincides with the real value λ_0 of the image position and the QL estimate in Equation (9) is consistent.

Let $S_m = \sup\limits_{\lambda} S(\lambda,\lambda_0) = S(\lambda,\lambda_0) = \frac{2}{N_0}\iint\limits_{\Omega_S(0)} f(x,y)\times$ $\times g(x,y)dxdy$ denote the maximum value of the signal component(12)and $\sigma_N^2 = \langle N^2(\lambda)\rangle = \frac{2}{N_0}\iint\limits_{\Omega_S(0)} g^2(x,y)dxdy$ denote the dispersion of the noise component in Equation (13). Taking into account the last representations, one can rewrite Equation (11) in the form

$$L(\lambda) = S_m\hat{S}(\lambda,\lambda_0) + \sigma_N\hat{N}(\lambda) = \\ = \sigma_N[\tilde{z}\hat{S}(\lambda,\lambda_0) + \hat{N}(\lambda)], \tag{15}$$

where

$$\hat{S}(\lambda,\lambda_0) = S(\lambda,\lambda_0)/S_m = \\ = \iint\limits_{\Omega_{\min}(\lambda,\lambda_0)} f(x-\lambda_0,y)g(x-\lambda,y)dxdy/ \\ \iint\limits_{\Omega_S(0)} f(x,y)g(x,y)dxdy, \tag{16}$$

$$\hat{N}(\lambda) = N(\lambda)/\sigma_N = \\ = \sqrt{\frac{2}{N_0}}\iint\limits_{\Omega_S(\lambda)} n(x,y)g(x-\lambda,y)dxdy/ \\ \sqrt{\iint\limits_{\Omega_S(\lambda)} g^2(x,y)dxdy}, \tag{17}$$

are the normalized signal component in Equation (16) and noise component in Equation (17), $\Omega_{\min}(\lambda,\lambda_0) = \Omega_S(\lambda)\cap\Omega_S(\lambda_0)$, $\tilde{z}^2 = S_m^2/\sigma_N^2 = z^2K_{fg}^2$ is the power signal-to-noise ratio (SNR) at the output of the QL receiver,

$$z^2 = \frac{2}{N_0}\iint\limits_{\Omega_S(0)} f^2(x,y)dxdy \tag{18}$$

is the power SNR at the output of the ML receiver while Equation (10) is satisfied (i.e. the image intensity distributions coincide) and

$$K_{fg} = \iint\limits_{\Omega_S(0)} f(x,y)g(x,y)dxdy/ \\ \sqrt{\iint\limits_{\Omega_S(0)} f^2(x,y)dxdy\iint\limits_{\Omega_2(0)} g^2(x,y)dxdy} \tag{19}$$

is the value that characterizes the difference between the forms of intensities of the received and the reference images.

The noise component in Equation (17) is realization of the centered Gaussian random process with the correlation function

$$K(\lambda_1,\lambda_2) = \langle\hat{N}(\lambda_1)\hat{N}(\lambda_2)\rangle = \\ = \iint\limits_{\Omega_{\min}(\lambda_1,\lambda_2)} g(x-\lambda_1,y)g(x-\lambda_2,y)dxdy/ \\ \iint\limits_{\Omega_S(0)} g^2(x,y)dxdy. \tag{20}$$

In the case of the optimal reception, functions in Equations (16) and (20) coincide, that is,

$$\hat{S}(\lambda_1,\lambda_2)|_{f=g} = K(\lambda_1,\lambda_2)|_{f=g} \tag{21}$$

for $\lambda = \lambda_1, \lambda_0 = \lambda_2$.

If value of the SNR $\tilde{z}$ is big enough, then the characteristics of the estimation algorithm in Equation (9) are defined by the behavior of the signal function in the small neighborhood of the real value λ_0 of the image position. The signal function in Equation (16) is then expanded into the Taylor series by the variable λ in the neighborhood of the point λ_0 and only the term containing the first derivative is taken into account there. According to (16), the signal function is continuously differentiable to both the right and the left of the neighborhood of the point λ_0, excluding the point $\lambda = \lambda_0$ where the derivative has the discontinuity of the first kind. Therefore, expansion of the function (16) has the form

$$\hat{S}(\lambda,\lambda_0) = 1 + \\ + \begin{cases} d_1(\lambda-\lambda_0) + o(|\lambda-\lambda_0|) & \lambda < \lambda_0, \\ -d_2(\lambda-\lambda_0) + o(|\lambda-\lambda_0|) & \lambda > \lambda_0, \end{cases} \tag{22}$$

where

$$d_1 = d\hat{S}(\lambda,\lambda_0)/d\lambda|_{\lambda=\lambda_0-0}, \\ d_2 = d\hat{S}(\lambda,\lambda_0)/d\lambda|_{\lambda=\lambda_0+0}, \tag{23}$$

and $o(|\lambda-\lambda_0|)$ denotes the higher-order infinitesimal terms compared to $|\lambda-\lambda_0|$.

Let, for example, the area , occupied by the image and set by the indicator $I(x,y)$, has the form shown in Fig. 1. Then, one projects this area on the axis *Oy*. Here $y_{\min}$, $y_{\max}$ are the minimum and maximum values of the y coordinate of the projection of the area $\Omega_S(0,0)$ on the ordinate axis, respectively. Now, the minimum and maximum values of the coordinate on the axis *Oy* on the border of the area $\Omega_S(0,0)$ are denoted as points *A* and *B*, respectively, while the parametric descriptions of the left

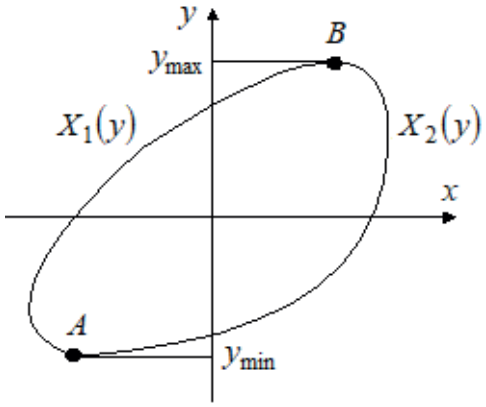

Figure 1 *The type of the area occupied by the image*

and right parts of the border of the area occupied by the image relative to the line AB are described as $X_1(y)$ and $X_2(y)$, respectively.

Using the introduced notations (see Figure 1), one can rewrite the signal function in Equation (16) in the form

$$\hat{S}(\lambda,\lambda_0) = \int_{y_{min}}^{y_{max}} \int_{X_1(y)+\max(\lambda,\lambda_0)}^{X_2(y)+\min(\lambda,\lambda_0)} f(x-\lambda_0,y)g(x-\lambda,y)dxdy \Big/ \iint_{\Omega S(0)} f(x,y)g(x-\lambda,y)dxdy. \quad (24)$$

Differentiating (24) by the variable λ and taking into account the finite size of the image existence area, one obtains expressions for the expansion coefficients in Equation (22):

$$d_i = (-1)^{i+1} \int_{y_{min}}^{y_{max}} \left\{ - \int_{X_1(y)}^{X_2(y)} f(x,y)\frac{\delta g(x,y)}{\delta x}dx + f(X_2(y),y)g(X_2(y),y)\delta_{1i} - f(X_1(y),y)\cdot g(X_1(y),y)\delta_{2i} \right\} dy \Big/ \iint_{\Omega S(0)} f(x,y)g(x-\lambda,y)dxdy, \quad (25)$$

where δ_{ij} is the Kronecker delta symbol. In practice, different combinations of types of intensity distribution of the real and presupposed (reference) images are possible. Therefore, carrying out the integration of Equation (25) by parts, one can present the expansion coefficients in Equation (25) in an alternative way:

$$d_i = (-1)^{i+1} \int_{y_{min}}^{y_{max}} \left[- \int_{X_1(y)}^{X_2(y)} g(x,y)\frac{\delta f(x,y)}{\delta x}dx + f(X_1(y),y)g(X_1(y),y)\delta_{1i} - f(X_2(y),y)\cdot g(X_2(y),y)\delta_{2i} \right] dy \Big/ \iint_{\Omega S(0)} f(x,y)g(x,y)dxdy, \quad (26)$$

Now are considered several special cases of the intensity distribution. If $g(x,y) = \text{const}$ and $f(x,y) \neq \text{const}$, then, for the expansion coefficients in Equation (23), Equation (25) is convenient because the integral by the variable x is reduced to zero and one gets

$$d_i = (-1)^{i+1} \frac{\int_{y_{min}}^{y_{max}} \left[f(X_2(y),y)g(X_2(y),y)\delta_{2i} - f(X_1(y),y)g(X_2(y),y)\delta_{1i} \right] dy}{\iint_{\Omega S(0)} f(x,y)g(x,y)dxdy}. \quad (27)$$

When $f(x,y) = \text{const}$ and $g(x,y) \neq \text{const}$, it is convenient to determine the expansion coefficients (23) of the signal function according to Equation (26) as follows

$$d_i = (-1)^{i+1} \frac{\int_{y_{min}}^{y_{max}} \left[f(X_1(y),y)g(X_1(y),y)\delta_{1i} - f(X_2(y),y)g(X_2(y),y)\delta_{2i} \right] dy}{\iint_{\Omega S(0)} f(x,y)g(x,y)dxdy}. \quad (28)$$

In the case of the optimal reception, the intensity distributions of the received and reference images coincide, that is, Equation (10) is satisfied and the expansion coefficients in Equation (23) of the signal function take the form

$$d_1 = d_2 = \int_{y_{min}}^{y_{max}} [f^2(X_1(y),y) + f^2(X_1(y),y)]dy \Big/ 2\iint_{\Omega S(0)} f^2(x,y)dxd. \quad (29)$$

The same result has been obtained in [10].

Now consider properties of the correlation function in Equation (20). Taking into account equality in Equation (21) of the signal in Equation (16) and correlation in Equation (20) functions under $f(x,y) = g(x,y)$, one can obtain an asymptotic expansion in Equation (20), while $|\lambda_2 - \lambda_1| \to 0$ as a special case of Equation (22). By substituting $g(x,y)$ instead of $f(x,y)$ in Equation (29), for the expansion coefficients in Equation (22) one gets

$$d_1 = d_2 = \int_{y_{min}}^{y_{max}} [g^2(X_1(y),y) + g^2(X_1(y),y)]dy \Big/ 2\iint_{\Omega S(0)} g^2(x,y)dxdy, \quad (30)$$

while $d_0 > 0$. Therefore, if $|\lambda_2 - \lambda_1| \to 0$, then the correlation function (20) allows the following asymptotic representation:

$$K(\lambda_1,\lambda_2) = \hat{S}(\lambda_1,\lambda_2)|_{f=g} = \\ = 11 + d_0|\lambda_2 - \lambda_1| + o(|\lambda_2 - \lambda_1|). \quad (31)$$

If intensity of the reference image is constant, that is, $g(x,y) = \text{const}$, then $d_0 = l_y/G_s$, where $l_y = y_{\max} - y_{\min}$ is the length of the image projection on the axis *Oy* (see Fig. 1), G_s is the image area [10]. While $|\lambda_2 - \lambda_1|$ increases, the correlation function in Equation (20) decreases and becomes zero, if $|\lambda_2 - \lambda_1| > l_x$. Here l_x is the length of the image projection on the axis *Ox*.

In view of the above, one can conclude that the decision statistics in Equation (15) of the QL estimation algorithm in Equation (9) is the Gaussian random process, for which the mathematical expectation and the correlation function, under conditions of high a posteriori accuracy, allow the representations in Equations (22) and (31), respectively. The statistical properties of such a process are studied in details in [10, 15]. Taking into account Equation (22), relations in Equation (14) conditioning the consistency of the QL estimate in Equation (9), can be rewritten in a more convenient form: $S_m > 0$, $d_i > 0$, $i = 1,2$. Thus, the conditions in Equations (14) are satisfied and the QL estimate in Equation (9) is consistent, if for all $y \in [y_{\min}, y_{\max}]$ the following inequalities hold:

$$\iint\limits_{\Omega_s(0)} f(x,y)g(x,y)dxdy > 0, \quad (32)$$

$$-f(X_1(y),y)g(X_1(y),y) < \\ < \int\limits_{X_1(y)}^{X_2(y)} g(x,y)\frac{\partial f(x,y)}{\partial x}dx < \quad (33) \\ < f(X_2(y),y)g(X_2(y),y).$$

5 The characteristics of the quasi-likelihood estimate of the image position

Next, one seeks characteristics of the image position QL estimate in Equation (9), assuming that this estimate is consistent. Taking into account the set properties of the signal in Equation (22) and correlation in Equation (31) functions, the conditional bias $b(\hat{\lambda}|\lambda_0) = \langle \hat{\lambda} - \lambda_0 \rangle$ and variance $V(\hat{\lambda}|\lambda_0) = \langle (\hat{\lambda} - \lambda_0)^2 \rangle$ of the reliable estimate in Equation (9) can be found by applying the local Markov approximation method as it is described in [16-17]. As a result, one gets

$$b(\hat{\lambda}|\lambda_0) = \frac{z_1^2 R(R+2) - z_2^2(2R+1)}{z_1^2 z_2^2 (R+1)^2}, \quad (34)$$

$$V(\hat{\lambda}|\lambda_0) = 2\frac{z_1^4 R(2R^2+6R+5) + z_2^4(5R^2+6R+2)}{z_1^4 z_2^4 (R+1)^3}, \quad (35)$$

where

$$R = d_1/d_2, \ z_1^2 = \tilde{z}^2 d_i^2/d_0, \ i = 1,2. \quad (36)$$

By substituting Equation (36) into Equations (34) and (35), for the required bias and variance, one obtains

$$b(\hat{\lambda}|\lambda_0) = \frac{d_0(d_1^2 - d_2^2)}{\tilde{z}^2 d_1^2 d_2^2}, \quad (37)$$

$$V(\hat{\lambda}|\lambda_0) = \frac{2d_0^2}{\tilde{z}^4} \cdot \\ \cdot \frac{2(d_1^6 + d_2^6) + 4d_1d_2(d_1^4 + d_2^4) + d_1^2 d_2^2 (d_1^2 + d_2^2) - d_1^3 d_2^3}{d_1^4 d_2^4 (d_1 + d_2)^2}. \quad (38)$$

If shapes of the received and the reference images coincide (the condition in Equation (10) is satisfied), then according to Equations (29) and (30), $d_1 = d_2 = d_0$ and the bias in Equation (37) and variance in Equation (38) take the form

$$b(\hat{\lambda}|\lambda_0) = 0, \quad V(\hat{\lambda}|\lambda_0) = 13/2z^4 d_0^2, \quad (39)$$

respectively.

It should be noted that these expressions coincide with characteristics of the ML estimate of the image position obtained in [10].

Then, one considers, for example, estimate of the rectangular image position. Let in the observation area of the image be present a rectangle with sides l_x and l_y, parallel to the axes *Ox* and *Oy*, respectively. In this case, one selects the coordinate system so that its origin is located at the intersection of the rectangle diagonals. One assumes that the image intensity is described by a linear function that increases in the direction of the angle θ with the side l_x (axis *Ox*):

$$f(x,y) = \\ = AS_0\left[\frac{(q-1)(x\cos\theta + y\sin\theta)}{l_x\cos\theta + l_y\sin\theta} + \frac{q+1}{2}\right]. \quad (40)$$

Here, the multiplier

$$A = \left[\frac{(q-1)^2}{12}\frac{l_x^2\cos^2\theta + l_y^2\sin^2\theta}{(l_x\cos\theta + l_y\sin\theta)^2} + \left(\frac{q+1}{2}\right)^2\right]^{-1/2}$$

is introduced to provide the constancy of the image energy for different values of q and θ. The value $q = s_{\max}/s_{\min}$ characterizes the slope, while S_0 - the magnitude of the change in the image intensity; $s_{\max} = \max f(x,y)$, $s_{\min} = \min f(x,y), x,y \in \Omega$, are the maximum and minimum intensity values, respectively. For a uniform image that has the same area and shape as the non-uniform one, the slope is $q = 1$, so that $f(x,y) = S_0$. One chooses the uniform image with the intensity $g(x,y) = S_0$ as the expected one. This corresponds to the case when a receiver synthesized for estimating the position of a uniform image is applied for the position estimate of a non-uniform image in Equations (1), (40). By substituting Equation (40) and $g(x,y) = S_0$ into Equation (27), one finds expressions for the expansion coefficients in Equations (22), (31)

$$d_0 = 1/l_x, \ d_1 = (1+a)/l_x, d_2 = (1-a)/l_x, \\ a = \frac{q-1}{q+1}\frac{\cos\theta}{\cos\theta + \gamma\sin\theta}, \gamma = l_y/l_x. \quad (41)$$

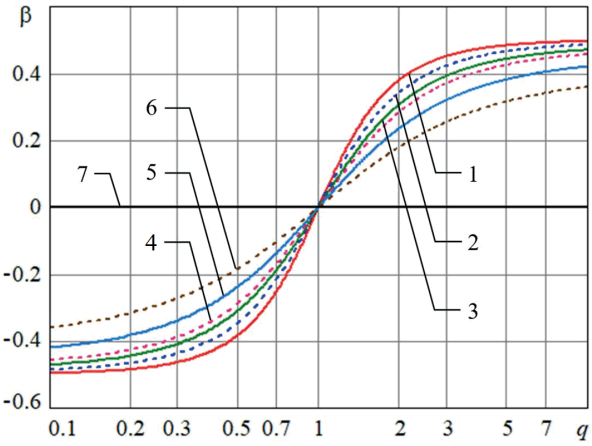

Figure 2 *Dependences of the normalized bias of the image position QL estimate*

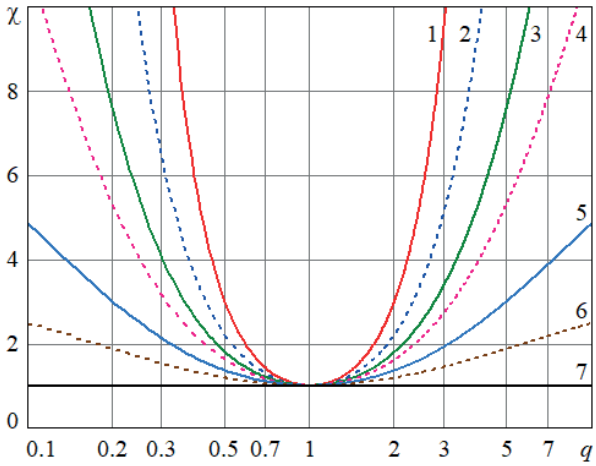

Figure 3 *Dependences of the loss in the accuracy of the image position QL estimate due to the ignorance of the image intensity*

Taking into account Equation (41), expressions for estimation characteristics in Equations (37) and (38) take the form

$$b(\hat{\lambda}|\lambda_0) = 4al_x/\tilde{z}^2(a^2-1)^2, \tag{42}$$

$$V(\hat{\lambda}|\lambda_0) = \frac{l_x^2}{2\tilde{z}^4}\frac{13+15a^4+101a^2-a^6}{a^8-4a^6+6a^4-4a^2+1}. \tag{43}$$

For the case when $q=1$ in Equations (41)-(43), one obtains expressions for the bias and the variance of the ML estimate of the uniform image position that coincide with the expressions in Equation (39):

$$b(\hat{\lambda}|\lambda_0) = 0,\ V_0(\hat{\lambda}|\lambda_0) = 13l_x^2/2z^4, \tag{44}$$

respectively.

Comparing Equations (42) and (43) to Equation (44), one can estimate influence of the non-uniformity of the image brightness distribution upon the accuracy of the QL estimate of the image position. Unlike the ML estimate, the QL estimate is biased as it follows from Equation (42). While the deviation of the parameter q from unity increases, the absolute magnitude of the estimate bias increases too. When the bias is a significant part of the mean-root-square error, it significantly reduces the accuracy of the estimate. Therefore, one introduces the normalized bias

$$\beta(\hat{\lambda}|\lambda_0) = b(\hat{\lambda}|\lambda_0)/\sqrt{V(\hat{\lambda}|\lambda_0)}, \tag{45}$$

that shows what proportion of the mean-root-square is the bias of the QL estimate.

Graphs of dependence of the normalized bias in Equation (45) of the QL estimate upon the parameter q under $\gamma=1$ and the varied values of the parameter θ are presented in Figure 2. Here, the curve 1 corresponds to value $\theta=0$, the curve 2 - to $\theta=\pi/16$, the curve 3 - to $\theta=\pi/8$, the curve 4 - to $\theta=\pi/6$, the curve 5 - to $\theta=\pi/4$, the curve 6 - to $\theta=\pi/3$, the curve 7 - to $\theta=\pi/2$ (the last curve coincides with the abscissa axis). From Figure 2 can be seen that the QL estimate is unbiased under $q=1$. If $q\neq 1$, then, for the same value of q, accuracy of the estimate decreases with increasing θ, and that corresponds to the increasing degree of difference between the received and the presupposed images.

In order to characterize the loss in accuracy of the QL estimate, while comparing it to the same kind of loss in case of the ML estimate, one introduces the relation

$$\chi(\hat{\lambda}|\lambda_0) = V(\hat{\lambda}|\lambda_0)/V_0(\hat{\lambda}|\lambda_0), \tag{46}$$

where $V(\hat{\lambda}|\lambda_0)$ and $V_0(\hat{\lambda}|\lambda_0)$ are determined in Equations (43) and (44), respectively.

In Figure 3, the graphs demonstrate dependence of the loss in the QL estimate accuracy (46) upon the parameter q under $\gamma=1$ and the varied values of the parameter θ. Here the notations coincide with the ones introduced in Figure 2. From Figure 3, it follows that under $q=1$, there is no loss in the QL estimate accuracy. However, under the fixed $q\neq 1$, the loss increases with the increasing θ and that corresponds to the increasing degree of difference between the intensities of the received and the reference (presupposed) images. When the value q increases and the value θ is fixed, the loss increases.

6 Conclusion

Synthesis and analysis of the rather simple QL algorithm have been carried out for estimating the position of the image with the unknown intensity distribution. As a result, the expansion is found of the signal function of the decision statistics in the neighborhood of the image position real value. Expressions are obtained for the bias and variance of the resulting estimate of the measured image coordinate. The dependence of the estimate characteristics upon the non-uniformity of the image intensity distribution is examined on an example of an image with the set intensity distribution. The relations

obtained allow determining the loss in accuracy of the image position estimate due to a priori ignorance of the image intensity distribution.

In the case when the intensity profiles of the received and the reference images differ significantly, so that the loss in the QL estimate accuracy becomes significant, an adaptation of the estimation algorithm, by the unknown intensity profile that leads to the improvement in the accuracy of the image position estimate, can be applied. One of the possible ways to implement adaptation is to expand the intensity profile function in terms of an orthogonal function system basis with a further estimation of the expansion coefficients. The nonparametric estimate of the intensity profile can also be used [18].

These results can be used in design of the measuring systems for object monitoring in the field of transport services, security, process and production control, etc.

Acknowledgement

This study was financially supported by the Ministry of Education and Science of the Russian Federation (research project No. FSWF-2020-0022).

References

[1] DOBRUCKY, B., MARCOKOVA, M., POKORNY, M., SUL, R. Prediction of periodical variable structure system behaviour using minimum data acquisition time. In: 26th IASTED International Conference on Modelling, Identification, and Control (MIC): proceedings. Calgary: ACTA Press, 2007. ISBN 978-0-8898-6633-1, p. 440-445.

[2] OSTROVITYANOV, R. V., BASALOV, V. F., BARTON, W. F., BARTON, D. K. *Statistical theory of extended radar targets*. 1. ed. Norwood, MA: Artech House, 1985. ISBN 0890061440.

[3] REFREGIER, P., GOUDAIL, F. *Statistical image processing techniques for noisy images. An application-oriented approach*. New York: Springer, 2004. ISBN 1461346924.

[4] FIEGUTH, P. *Statistical image processing and multidimensional modeling*. New York: Springer, 2011. ISBN 1441972935.

[5] TRIFONOV, A. P., KUTSOV, R. *Dynamic image processing* (in Russian). Moscow: LAP Lambert Academic Publishing, 2011. ISBN 3845474068.

[6] BYCHKOV, A. A., PON'KIN, V. A. Detection of random images of lengthy in space objects shadowing the background. *Avtometriya* [online]. 1992, **28**(6), p. 33-40 [accessed 1992-09-01]. ISSN 0320-7102. Available from: https://www.iae.nsk.su/images/stories/5_Autometria/5_Archives/1992/4/33-40.pdf

[7] TRIFONOV, A. P., PRIBYTKOV, Y. N., CHERNOYAROV, O. V., MIKHAILOV, B. B. Estimating the image area with unknown parameters of the image and background. *Journal of Communications Technology and Electronics* [online]. 2015, **60**(11), p. 852-859 [accessed 2015-08-18]. ISSN 1064-2269. Available from: https://doi.org/10.1134/S1064226915080185

[8] TRIFONOV, A. P., PRIBYTKOV, Y. N. Quasi-deterministic image detection in the presence of background with unknown parameters. *Avtometriya* [online]. 2002, **38**(6), p. 19-31 [accessed 2002-09-01]. ISSN 0320-7102. Available from: https://www.iae.nsk.su/images/stories/5_Autometria/5_Archives/2002/4/19-31.pdf

[9] TRIFONOV, A. P., SAVIN, S. A. Effectiveness of detection of images with unknown position. *Radioelectronics and Communications Systems* [online]. 2006, **49**(12), p. 1-8 [accessed 2019-09-30]. ISSN 0735-2727. Available from: https://doi.org/10.3103/S0735272706090019

[10] TRIFONOV, A. P., SAVIN, S. A. Effectiveness of detection and estimation of position of heterogeneous image. *Radioelectronics and Communications Systems* [online]. 2007, **50**(16), p. 647-656 [accessed 2007-12-30]. ISSN 0735-2727. Available from: https://doi.org/10.3103/S0735272707120011

[11] VAN TREES, H. L., BELL, K. L., TIAN, Z. *Detection, estimation, and modulation theory. Part I. Detection, estimation, and filtering theory*. 2. ed. New York: Wiley, 2013. ISBN 9780470542965.

[12] CHERNOYAROV, O. V., VACULIK, M., SHIRIKYAN, A., SALNIKOVA, A. V. Statistical analysis of fast fluctuating random signals with arbitrary-function envelope and unknown parameters. Communications - Scientific Letters of the University of Zilina [online]. 2015, 17(1A), p. 35-43 [accessed 2015-04-30]. ISSN 1335-4205. Available from: http://komunikacie.uniza.sk/index.php/communications/article/view/410

[13] CHERNOYAROV, O. V., BREZNAN, M. Optimal and quasioptimal algorithms of distinction of the compressed images in bases of orthogonal polynomials. *Communications - Scientific Letters of the University of Zilina* [online]. 2012, **14**(3), p. 22-26 [accessed 2012-06-30]. ISSN 1335-4205, eISSN 2585-7878. Available from: http://komunikacie.uniza.sk/index.php/communications/article/view/742

[14] CHERNOYAROV, O. V., BREZNAN, M., TEREKHOV, A. V. Restoration of deterministic and interference distorted signals and images with use of the generalized spectra in bases of orthogonal polynomials and functions. *Communications - Scientific Letters of the University of Zilina* [online]. 2013, **15**(2A), p. 71-77 [accessed 2013-07-31]. ISSN 1335-4205, eISSN 2585-7878. Available from: http://komunikacie.uniza.sk/index.php/communications/article/view/658

[15] TRIFONOV, A. P., SMORGONSKY, A. V. Quasiprobable estimation of arrival instant of finite signal. *Radioelectronics and Communications Systems* [online]. 2008, **51**(1), p. 40-49 [accessed 2008-01-31]. ISSN 0735-2727. Available from: https://doi.org/10.3103/S0735272708010068

[16] CHERNOYAROV, O. V., ZAKHAROV, A. V., TRIFONOV, A. P., SALNIKOVA, A. V., MAKAROV, A. A., The common approach to calculating the characteristics of the signal parameters joint estimates under the violation of the decision statistics regularity conditions. *Engineering Letters* [online]. 2020, **28**(2), p. 492-503 [accessed 2020-05-28]. ISSN 1312-885X. Available from: http://www.engineeringletters.com/issues_v28/issue_2/index.html

[17] CHERNOYAROV, O. V., SALNIKOVA, A. V., ROZANOV, A. E., MARCOKOVA, M. Statistical characteristics of the magnitude and position of the greatest maximum of Markov random process with piecewise constant drift and diffusion coefficients. *Applied Mathematical Sciences* [online]. 2014, **8**(147), p. 7341-7357 [accessed 2014-10-22]. ISSN 1312-885X. Available from: https://doi.org/10.12988/ams.2014.49740

[18] PCHELINTSEV, E. A., PERGAMENSHCHIKOV, S. M. Model selection method for efficient signals processing from discrete data. In: 31st European Modeling and Simulation Symposium (EMSS): proceedings. Genoa: Dime University of Genoa, 2019. ISBN 978-8-8857-4126-3, p. 90-95.